



A tunable controlled-release urea fertilizer coated with a biodegradable polyurethane-nanoclay composite layer

Kannika Sitthisuwannakul, Kanittha Boonpavanitchakul , Thanakorn Wirunmongkol, Pennapa Muthitamongkol, Wiyong Kangwansupamonkon

Received: 15 April 2022 / Revised: 8 July 2022 / Accepted: 17 July 2022
© American Coatings Association 2022

Abstract To minimize a loss of urea to the environment and also control a release activity, a tunable and controlled-release urea fertilizer (TCRF) was created. Composite coating layers of the TCRF were synthesized using a composite of nanoclay (B27), and a linseed oil-modified polyurethane resin (BURNOCK® UL65). The concentration of B27 nanoclay was varied from 0, 3, 5 and 10 wt% and called TCRF, TCRF-3, TCRF-5 and TCRF-10, respectively. Firstly, nanocomposite free-standing films (NFs) with 0, 0.5, 1, 3, 5 and 10 wt% of B27 were synthesized and tested to demonstrate the mechanical properties of the coating layer. When the B27 clay content increased, the Young's modulus and yield strength were increased. On the other hand, the elongation at break was decreased. NFs were also characterized by XRD and

TEM, which showed a partial exfoliated nanocomposite character. The water contact angle measurement showed that all NFs had hydrophobicity properties (87°–90° contact angle). Moreover, the microorganism degradability test showed that the NFs degraded at $37 \pm 2^\circ\text{C}$ and $58 \pm 2^\circ\text{C}$ in manure, a common agriculture media. The study on coated urea fertilizers found that the thickness of all TCRFs layers is around 52–54 μm . The nitrogen release profiles of the TCRF at 60°C in water as a predictive analytic model were investigated using an elemental analyzer that is a pathway analysis method to understand the release profiles of the TCRFs. All release profiles fitted well with the sigmoidal model, which was suitable for a common plant growth. The profiles gave diffusion coefficients (D) in the range of 49–69 $\mu\text{m}^2 \text{h}^{-1}$ and presented an inverse trend to the yield strength of the NFs. The investigation demonstrated that B27 played an important role in tuning the strength of the coating layers that affected the urea release to the plants and the environment.

Supplementary Information The online version contains supplementary material available at <https://doi.org/10.1007/s11998-022-00688-w>.

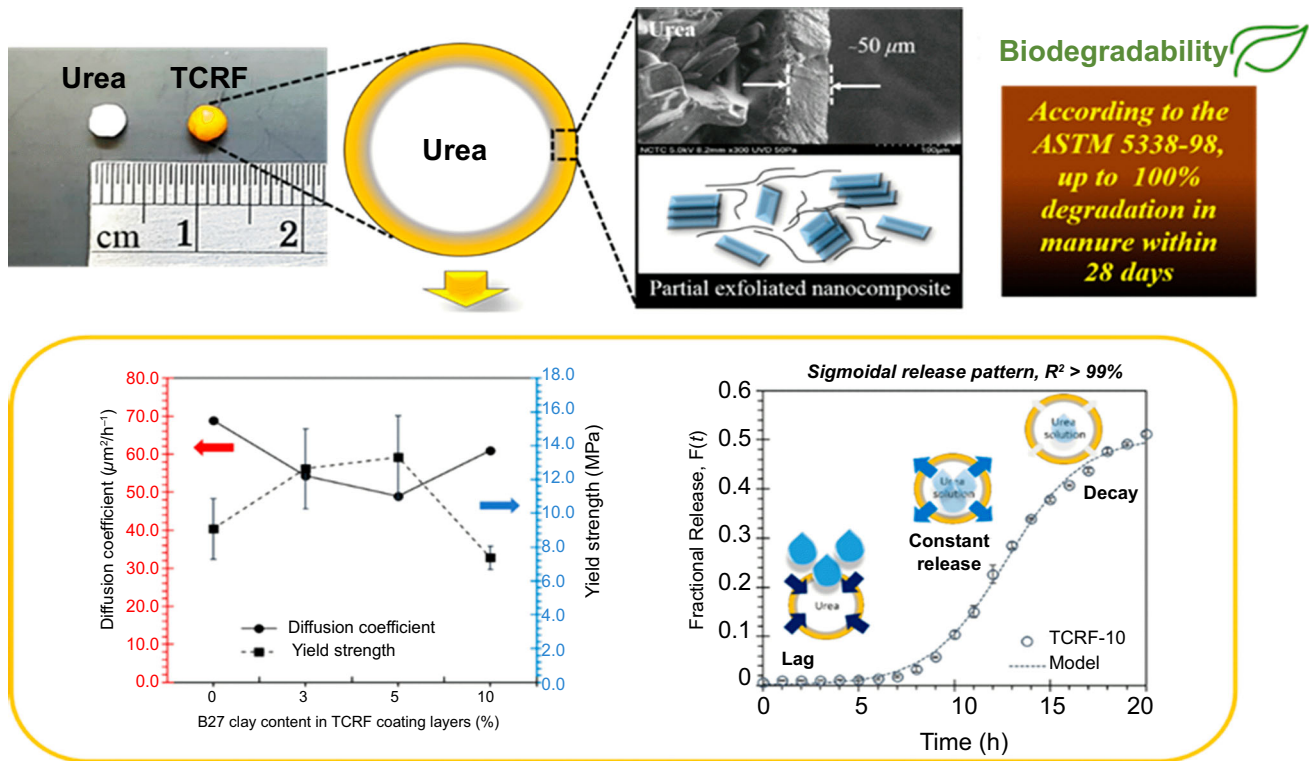
K. Sitthisuwannakul, K. Boonpavanitchakul (✉),
T. Wirunmongkol, W. Kangwansupamonkon (✉)
National Nanotechnology Center, National Science and
Technology Development Agency, 111 Thailand Science
Park (TSP), Phahonyothin Road, Khlong Nueng, Khlong
Luang, Pathum Thani 12120, Thailand
e-mail: kanittha@nanotec.or.th

W. Kangwansupamonkon
e-mail: wiyong@nanotec.or.th

P. Muthitamongkol
National Metal and Materials Technology Center, National
Science and Technology Development Agency, 114
Thailand Science Park (TSP), Phahonyothin Road, Khlong
Nueng, Khlong Luang, Pathum Thani 12120, Thailand

W. Kangwansupamonkon
AFRST, The Royal Society of Thailand, Sanam Sueapa,
Dusit, Bangkok 10300, Thailand

Graphical abstract



Keywords Controlled-release fertilizer, Nanoclay composite, Sigmoidal equation, Biodegradable materials

Introduction

Urea is one of the most utilized fertilizers for supplying nitrogen (N) as an essential nutrient that plants require in large amount for growth and development. However, it is well known that the limitations of using the conventional urea fertilizer are losing of N to the soil and leaching it into the environment due to its high solubility in water.^{1–4} The release of excess nitrogen in the soil is not only detrimental to the environment but also lessens the efficiency of conventional urea.

This causes nutrient inefficiency in plant uptake resulting in reduced biomass production and adverse environmental impacts. A controlled-release urea fertilizer became an option because of its advantage in terms of minimizing rate of nitrogen release.^{5,6} Coated fertilizers are nutrient particles underneath coating layers to retard the nutrient release rate. These fertilizers are categorized into two types: mineral coating (e.g. sulfur) and polymer coating.⁷ Sulfur-coated fertilizers have been reported to have non-uniform coating layers resulting in a non-uniform nitrogen release profile.⁸ In contrast, a polymer coated fertilizer (PCF) is a nutrient core coated with a single

or multilayer polymer.^{9–11} An ideal PCF is a fertilizer coated with natural or semi-natural environmentally friendly macromolecules and affords the release profile that meets nutrient requirements for a model crop growth with a single application.¹² However, in the field of agriculture, the PCFs still need the prolonged-release nutrient for crop production.^{8,13}

Agricultural nitrogen (N) demand depends on crop species and soil conditions. Recently, a simulation of the N demand for a sugarcane production was investigated. Researchers also reported a model of the N demand for ratoon crops in cases of seasonal responsiveness to different climatic and management conditions.^{14,15} The result showed that all simulated N uptake profiles performed an average initial lag period followed by a rapid linear N release and then a decay period. The total N uptake increased when the sugarcane had a limited irrigation allocation or was rain-fed. For a maize plantation, the N release rate significantly affected the root exudation quantity and compositions, such as sugar, sugar alcohol and phenolic components.^{16–18} Most importantly, a forest category is the main explanatory factor of soil N variability both for the forest floor and the mineral soil layer.¹⁹ Due to the N requirement of an agricultural area differing from an individual plant growth demand, not only a slow release but also a tunable controlled-release urea fertilizer is needed.

To understand mechanisms of the nutrient release, many kinetic models were applied to the release patterns.^{9,20–22} The releasing rate of a PCF depended

on the characteristic features of the PCF such as shape of the PCF and environmental conditions including temperature and testing medium.^{23–25} In order to match the fertilizer usage with the plant nutrient uptake for the sustainable crop production, Shaviv et al. developed a mechanistic-mathematical model to describe the release using the diffusion mechanism, so called a sigmoidal model.^{26,27} The sigmoidal model explained that the release was controlled by mass transfer properties of the coating material, nutrient active properties and the thickness of the coating layer. According to the sigmoidal model, it described the “non-Fickian” nature of a cumulative release consisting of three stages: a lag period, a constant release, and a decay stage (shown in the graphical abstract). During the lag period, water penetrated into the granule and dissolved an active molecule via an osmotic water pressure across the coating layer. The lag period was the time needed to fill the internal voids of the granule with a critical water volume. This stage could be attributed to the time needed for the establishment of a steady stage between the flux of water entering the granule and the flux of solute leaving it. The second stage, the constant release, began with a critical volume of saturated solution occurring inside the PCF. The release rate remained constant until the equilibrium concentration presented. The final stage was the decay stage. The driving force for the release decreased and the release rate decayed when the internal concentration decreased to the continuing fluxes of the nutrient out.

Nanoclays or a layer-silicate nanoparticles were one of the best natural materials for polymer composites in order to control the nutrient releasing rate due to the advantages of good mechanical properties especially under a water barrier.^{28–30} In particular, a swelling clay, termed smectite such as montmorillonite (MMT) and hectorite clay, is composed of two tetrahedral (T) silicate sheets sandwiching with one octahedral (O) structure. The 2:1 of T:O ratio presented exchangeability of cations and cationic surfactants between the intercalating layer to adjust a width and the swelling ability of the nanoclay. Good swelling in the medium revealed a compatibility with the polymer system and also affected the nanocomposite categorization. Generally, there were three categories in terms of their structures and configurations; the conventional composites, intercalated nanocomposites and exfoliated nanocomposites. The mechanical performance of the polymer–clay nanocomposite dramatically depended on the nanocomposite configuration category. Nanoclay usually improved the tensile strength of polymers causing the degree of the intercalation/exfoliation and had a great impact to the Young’s modulus and an elongation at break. It had been reported that the intercalated or the exfoliated clay nanocomposites were used as controlling materials and blended with nutrients to control the releasing nutrient rate.^{31,32} Herein, the stronger the coating layer, the lower the nutrient releasing rate.

To the best of our knowledge, we created a novel controlled-release urea fertilizer (TCRF) that was also tunable by integrating a biodegradable polymer-nanoclay composite coating layer. A polyurethane modified long-oil alkyd resin was used as a biodegradable polymer media. An organic modified nanoclay (B27) called hectorite clay was used in the nanocomposite coating layer. TCRF was prepared by a pan coating process, which was an inexpensive technique and easy to modify for commercial manufacture. It is well known that the existence of nano-clay is a key factor to prove the mechanical property. Thus, the tunable property depended on the strength of the coating layer varied in the amount of the B27 content. However, there is little information to discuss in terms of controlled release fertilizer. Besides, a study of the nitrogen release pattern from TCRF is very essential to understand the release characteristics of TCRF. This study offers the sigmoidal pattern which appropriates with the active nutrient plant uptake demand. The nitrogen release test and kinetic study of TCRF are evaluated at 60°C as an accelerated condition. This condition is a predictive analytic model that can perform the behavior and performance of polymer nanoclay composite coating layer that are related between nitrogen release and nanoclay content as the definition of a characteristic parameter. Finally, this research provided directions for future research steps to overcome the nutrient loss risk of fertilizer that can be applied towards commercial application. This offered a high potential for agricultural applications of various plant species and soil conditions.

Materials and methods

Chemicals

Linseed oil-modified polyurethane resin, BURNOCK® UL65 (65% solid content) was supplied by Siam Chemical Industry Co., Ltd. (Bangkok, Thailand). Driers, Troymax™ Calcium 10NA and Troymax™ Manganese 10 were used as catalysts for the polymer curing and were from Koventure Co., Ltd (Samutprakan, Thailand). An unmodified montmorillonite (MMT) nanoclay was used to compare with an organic modified nanoclay B27. MMT nanoclay and B27 were from Brenntag Ingredients Public Co., Ltd (Bangkok, Thailand). B27 chemical composition was confirmed by wavelength dispersive X-ray fluorescence spectrometer, WDXRF (Bruker Axs, Germany: model S4 Pioneer) and the results are shown in Table S1. The results indicated main elements, Si and Mg of the hectorite clay. The BARCO® 100% AAA thinner from TOA Paint Co., Ltd (Samutprakan, Thailand.), which contained about 80% toluene, was used as a polymer solvent. Moreover, the deionized water, 18.2 MΩ-cm, PURELAB® Ultra Genetic Water Purifica-

tion Systems from ELGA LabWater, was used throughout this research.

Nanocomposite free-standing films (NFS) preparation

Nanocomposite films (NFs) to be used as a urea coating layer were synthesized and tested for mechanical properties. The amount of 0.5, 1, 3, 5 and 10 wt% the B27 nanoclay was varied with respect to the solid content of the resin and was slowly added to the 55 wt% of resin solution while being stirred at 800 rpm. The mixture was left overnight at the ambient temperature of 25°C. After that, 0.5 wt% Ca and 0.1 wt% Mn driers were added to the mixture and continually stirred for 15 min. The 12.00 g mixture was poured into the 7 × 15 cm silicone mold and dried in an oven at 100°C for 6 h to obtain nanocomposite free-standing films containing the intended wt% of the B27, labeled as NF for without the B27, NF-0.5, NF-1, NF-3, NF-5 and NF-10, respectively.

Biodegradability analysis of the NF

A biodegradability test was performed according to ASTM D5338-98 which determined the degree and rate of aerobic biodegradation of plastic materials on exposure to controlled-composting environment under laboratory conditions and designed to yield a percentage of conversion of carbon in the sample to carbon dioxide. In this research, a stable manure with 10^7 CFU g^{-1} total bacteria was used as inoculum while a cellulose microcrystalline and polyethylene samples were used as cellulose microcrystalline (R^+) and polyethylene (R^-) control samples, respectively. All samples were mixed with inoculum at 1 wt% and incubated at $37 \pm 2^\circ\text{C}$ and $58 \pm 2^\circ\text{C}$ for 28 days before detecting the CO_2 from the systems.

Tunable controlled-release urea fertilizer (TCRF) preparation

The B27 nanoclay resin mixture was prepared by stirring with a mechanical overhead stirrer (IKA, Germany: model RW20) before using as a coating material in a pan coating process (developed by NANOTEC, Thailand). The required amount of the B27 nanoclay was mixed with 1 kg of thinner. The resulting mixture was added to the 360 g of resin. This ratio resulted in about 12 wt% of the resin to the 2 kg of urea. Next, the resin mixture was stirred at 500 rpm for 2 h and slowed down to 130 rpm for 30 min to bleed microbubbles in the mixture. After that, 0.5 wt% Ca and 0.1 wt% Mn, were added to the mixture and continually stirred for 15 min before the following coating process.

In a pan coater, 2 kg of urea particles were first circulated at 8 rpm before slowly added the B27 nanoclay resin mixture. The average particle size of urea was approximate 3–4 mm. The initial drying with a blower at 65°C was performed. Afterward, the coated urea fertilizer was completely dried in the oven at 100°C for 6 h to receive the tunable controlled-release urea fertilizers (labeled as TCRF for without the B27, TCRF-3, TCRF-5 and TCRF-10 according to the percentage of the B27 nanoclay loading).

Characterizations

X-ray diffractometer, XRD Rigaku, Japan: model TTRAX III equipped with a CuK_α tube ($\lambda = 0.15406$ nm) was used to study the d -spacing in d_{001} plane of the original MMT and B27 nanoclays, including in the NFs. The analysis conditions: increment step 0.01° and 2θ from 1 – 10° were used. Furthermore, the morphologies of the NFs were studied by a transmission electron microscope, TEM (Jeol, Japan: model JEM 2100) using an accelerating voltage of 80 kV. Sample preparations were obtained via Leica EM UC7 ultra-microtome feeding of liquid nitrogen at -90°C resulting in 80 nm thickness of the NFs. After that, samples were placed onto copper grids and left in the ambient temperature for at least 24 h before TEM analysis.

To identify functional groups in the NFs, an attenuated total reflection Fourier transform infrared (ATR-FTIR) spectroscopy technique (Thermo-scientific, USA: model Nicolet 6700) was used in the range of 4000 to 500 cm^{-1} in the transmission mode acquired from 64 scans at a 4 cm^{-1} resolution. To investigate the mechanical properties of the NFs, a tensile testing was performed followed the ASTM D882: Standard Test Method For Tensile Properties Of Thin Plastic Sheet- ing. All of the NFs were prepared into a size of 2×10 cm prior to the test by a universal testing machine (Lloyd, USA: model LR 10 k). A water contact angle technique was used to determine the hydrophobicity of the NFs using a dynamic contact angle device (Dataphysics, Germany: model TC/TPC 150). The reported value was an average value of five measurements. A field emission scanning electron microscope, FESEM (Hitachi, Japan: model SU5000), operated at 5 kV was utilized to measure the TCRFs layer thicknesses and also characterize the morphology of the TCRFs coating layers before and after the nitrogen release test. All samples were placed on a carbon tape and sputter-coated with gold in a sputter coater (Quorum, Q150RS, UK) for 2 min. Thicknesses of the coating layer were determined from cross-sectional SEM images of samples using the public domain ImageJ software.

Nitrogen release test and kinetic study of TCRF

Glass containers which contained 5 g of the TCRFs in 20 cm³ of deionized water (DI) were prepared and placed in an oven at 60°C as an accelerated condition to obtain the whole state of the nitrogen release profile. Two-milliliter sampling was collected every hour for 20 h and the total nitrogen release was measured by an elemental analyzer, CHN Determinator (LECO, America: CHN628). According to Dumas method, also known as combustion method, this equipment is the most economical and innovative nitrogen/protein analyzer. In this analysis, the instrument was heated to 1,000°C and 50 ± 2 mg of sample was placed inside tin capsule, which was dropped into the furnace, where it was completely combusted. Thermal conductivity detection was used to measure nitrogen. Each set of experiments was repeated three times.

The kinetic study was analyzed using a mathematic model of the sigmoidal equation, equation (1). The $F(t)$ is the fractional release of nitrogen at time (t) while a , b , c and d are sigmoidal parameters.³³

$$F(t) = \frac{a - b}{1 + \exp\left(\frac{t-d}{c}\right)} + b \quad (1)$$

All experiments were carried out in triplicate, and an average value was reported. The static regression was applied to calculate the correlation coefficient (R^2) as a measure of the fit line reliability. Furthermore, important characteristic values according to the release pattern; lag time (t_{lag}), infection time (t_{inf}), inflection

slope (S_{inf}) and diffusion coefficient (D) were also observed as discussed in the literature.^{24,26,27,34}

The value of diffusion coefficient (D) through the polymer layer can be calculated according to equation (2), where h is the polymer layer thickness (μm).²⁴

$$D = \frac{h^2}{6 \times t_{lag}} \quad (2)$$

Results and discussion

Swelling performance and the characteristics of the nanoclays

For the polymer system compatibility, MMT and B27 performances in toluene were compared. The low angle XRD patterns of the MMT and the B27 nanoclays are shown in Fig. 1. The interlayer spacing could be calculated using the 2θ value of the d_{001} via Bragg's law. The MMT contained the d_{001} at 6.05° which corresponded to the d -spacing of 1.46 nm. On the other hand, the B27 provided a peak at 2θ equal to 4.80°, which corresponded to the d -spacing of 1.84 nm. The results clearly verified that the B27 contained a wider interlayer due to an organic molecule modification while the unmodified nanoclay MMT only had sodium ions or H₂O molecules inside. This is in good agreement with the literature.^{35,36} Furthermore, the inset of Fig. 1 shows a picture of the MMT and the B27 mixture in toluene media indicating a swelling feature and dispersing performance of these nanoclays. The MMT reveals a non-swelling and a non-dispersing feature in the clear solvent. It settled as dark gray precipitates at the bottom of the test-tube. In contrast, the B27 has dispersed and swelled on to the level slightly higher than that of the MMT, indicated by the dashed line. The larger volume of the B27 expressed the same hydrophobicity of B27 and the toluene, in the manner of like-dissolves-like interaction.^{35,37,38}

Figure 2 shows TEM images of (a) NF-MMT and (b) NF-3, which contain 3 wt% of the B27 in the resin. The NF-MMT gave large agglomerations of the MMT in the resin matrix indicating a poor dispersion. On the other hand, the NF-3 showed a dispersion of the B27 and some tactoid feature, paralleled intercalation pattern in the polymer matrix resulting in a partial exfoliated nanocomposite material. Due to the solvent and the polymer compatibility, the B27 was chosen to be a part of the urea coating layer in this research.

Chemical and physical properties of the NF

To characterize functional groups of the resin and a functional character of the NF containing B27, the ATR-FTIR was applied. Figure 3 shows ATR-FTIR spectra of NFs in the range of 500–2000 cm⁻¹

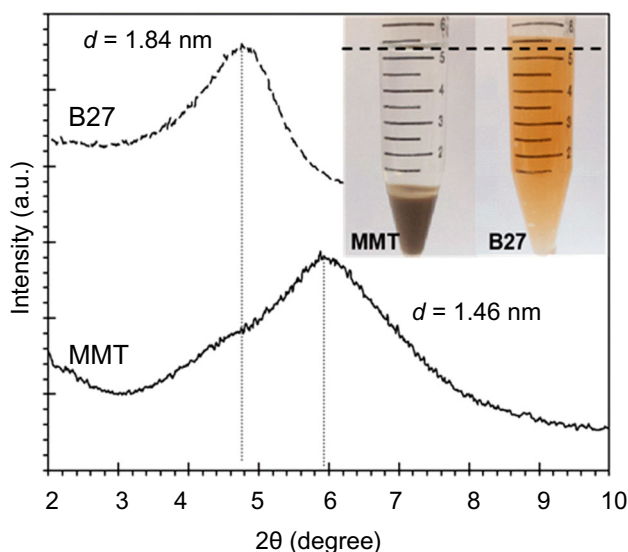


Fig. 1: XRD patterns of the MMT and the B27 nanoclay. The larger d -spacing of the B27 reveals the presence of the organic molecules in the modified nanoclay. The inset shows a higher volume of B27 indicating a swelling feature and a dispersity performance of the B27. The dashed line shows the level of the original toluene in containers

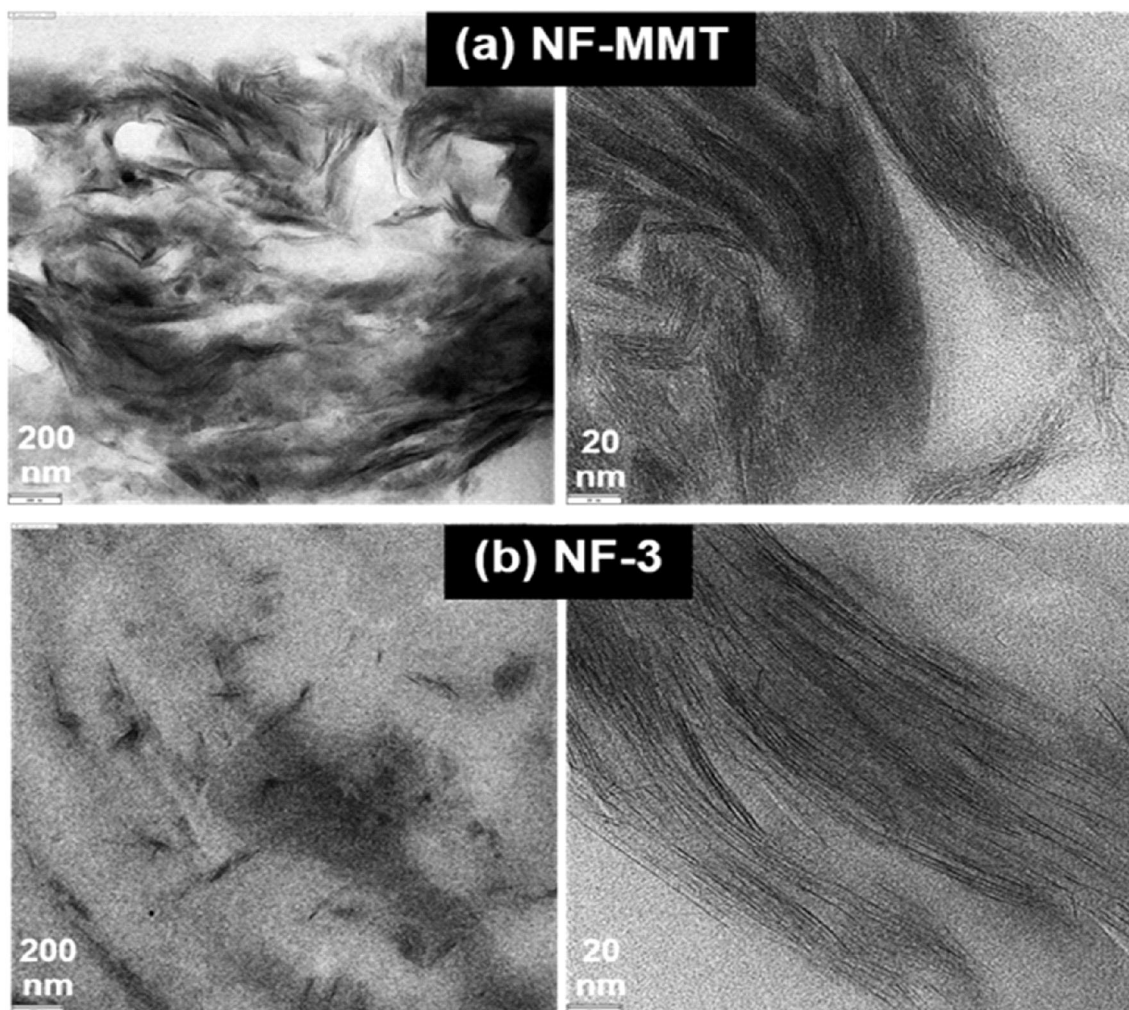


Fig. 2: TEM images of (a) NF-MMT and (b) NF-3, which contained 3 wt% of B27 in the polymer matrix. The images on the right are ten times higher magnification than those on the left

wavenumber. The peak at 1720 cm^{-1} corresponded to $-\text{C}=\text{O}$ stretching of an ester group. Transmittances at 1600 and 1530 cm^{-1} showed the $-\text{C}=\text{C}$ of aromatic and aliphatic unsaturated hydrocarbon, respectively. Furthermore, the adding of the B27 nanoclay content resulted in an increasing intensity of the peak at 993 cm^{-1} due to the rise of the Si–O–Si stretching vibration of the B27. XRD patterns shown in Fig. 4 corresponded to the d -spacing of d_{001} planes of the NFs containing different amount of the B27. The broader d_{001} peak characters at 2θ equals 1.80° (4.90 nm) of all NFs are different from the original B27, 2θ at 4.80° (1.84 nm). The result indicated that an intercalation/exfoliation and a disordered dispersion of the B27 occurred in the polymer matrix. In other words, the polymer penetrated in between the layers of B27 causing the d -spacing to become wider.

Mechanical and hydrophobic properties of the NFs are shown in Table 1. The mechanical properties included Young's modulus (MPa), yield strength (MPa) and % elongation at break. It showed that

increasing B27 resulted in higher Young's modulus and yield strength, and lower % elongation at break, which meant more rigid NFs. Generally, more contents of the B27 increased the Young's modulus and the yield strength because of a well-known advantage of reinforcement property of nanoclay. However, when the nanoclay content rises to the 10 wt%, some of the nanoclays agglomerate and induced some defects.³⁶ The higher rigidity caused lower flexibility of the sample resulting in the lower mechanical tensile strength. The results showed that NF, NF-0.5 and NF-1 had similar yield strength and % elongation at break, indicating that adding a small amount of the B27 did not affect overall strength of the NF. Furthermore, the water contact angle test of all NFs indicated the hydrophobicity listed in Table 1 as well. The water contact angle values of all NFs appeared to be in the same range of 87° – 90° , indicating similar hydrophobicity of all NFs. According to the results, the hydrophobic path of the resin base played an important role in the NF and the B27 did not have any significance even

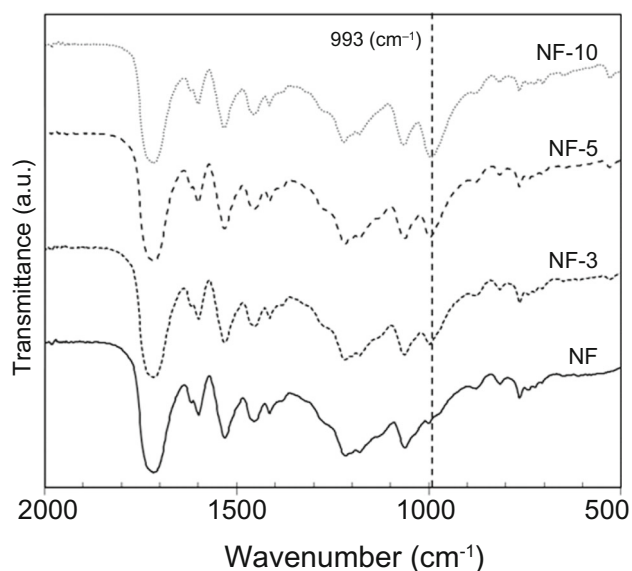


Fig. 3: ATR-FTIR spectra of NF nanocomposite films with 0, 3, 5 and 10 wt% of the B27 nanoclay. The increasing intensity of the peak at 993 cm^{-1} represents the increasing Si-O-Si stretching in the nanoclay

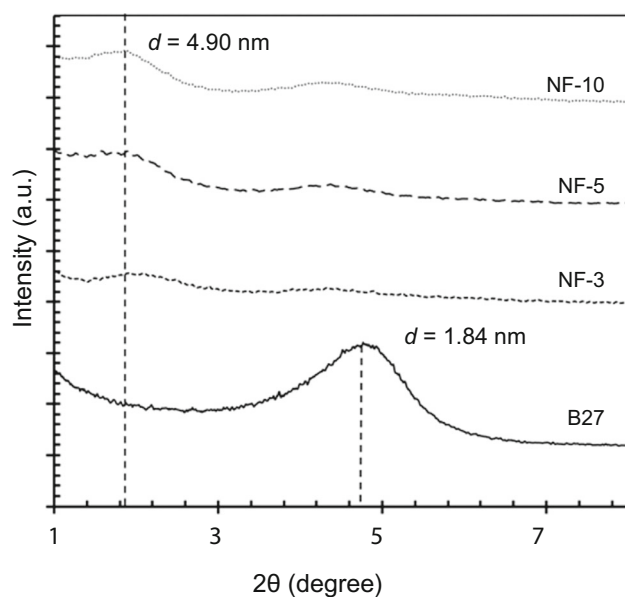


Fig. 4: XRD patterns of nanocomposite free films (NF), 3, 5 and 10 wt% of B27 in polymer film compared to the original B27 nanoclay

when the B27 content was raised to 10 wt%. Consequently, the B27 content in the NF films improved the mechanical properties of the films without having any impact on the hydrophobicity nor the initial water barrier property.

Biodegradable ability

Using biodegradable polymer is very important not only to prevent the early release of the steady stage of the nitrogen profile but also to be environmentally friendly.^{6,8,39} The percentages of biodegradation followed the ASTM 5338–98 standard of the NF and compared to the cellulose microcrystalline (R^+) as a biodegradable standard and the polyethylene sample (R^-) as a non-biodegradable standard are shown in Table 2. The experiments were performed at two temperature conditions: $37 \pm 2^\circ\text{C}$ and $58 \pm 2^\circ\text{C}$. The results indicate that the NF has around 50% biodegradation at 37°C and has completely degraded at 58°C within 28 days. It revealed that the resin used as the coating layer could be degraded by the microorganisms, especially the microorganisms in the stable manure generally used in agriculture. Even though only 50% biodegradation occurs at 37°C , the NF showed a possibility of complete degradation given a longer period of time.

Nitrogen release mechanism

In the study of release mechanisms, the 0.5 and 1 wt% of the B27 contents were ignored because they had similar mechanical strength as shown in Table 1. All TCRFs (TCRF, TCRF-3, TCRF-5 and TCRF-10) were tested for the nitrogen release in water media at 60°C as a predictive analytic model to evaluate the behavior and performance of polymer nanoclay composite coating layer, which related to the nutrient-tunable ability of TCRFs. The uncoated urea fertilizer was totally dissolved in water within 2 min in this testing condition. Release parameters and cumulative fractional release profiles of all TCRFs are shown in Fig. 5. In Fig. 5(a), the t_{lag} and S_{inf} were given by the release curve while the t_{inf} was from a derivative release curve, a release rate curve. Release patterns of all TCRFs shown in Fig. 5(b), indicated a similar S-curve pattern, which represented a lag period, a linear release and a decay phase. The correlation coefficient, R^2 , of the sigmoidal pattern indicated the well compatibility to the model, $> 99\%$ as shown in Table 3. The sigmoidal parameters of all nitrogen release patterns are shown in Table S2 (Supporting Information). The sigmoidal equation is one of the most important patterns that relates to the plant uptake, and consequently, TCRFs are suitable and adaptable for any plant growth.^{7,40} The sigmoidal equation for the multilayers, the initial stage becomes an important step for overall nutrient release. There are three steps that described the diffusion of the dissolved core nutrient. Firstly, the hydration penetrated to the permeable polymer layer and dissolved the soluble nutrient, urea. Secondly, the osmotic pressure developed and produced the linear release to the environment via the osmotic pathway. Lastly, the decay stage began because of the lower osmotic pressure from the

Table 1: Mechanical properties and contact angles of NF nanocomposite films

Sample	B27 clay content (wt%)	Mechanical properties			Contact angles (°) ^a
		Young's modulus (MPa)	Yield strength (MPa)	Elongation at break (%)	
NF	–	286 ± 64	9.1 ± 1.8	10.1 ± 2.3	87.9 ± 1.4
NF-0.5	0.5	345 ± 90	10.1 ± 0.7	8.2 ± 5.0	88.6 ± 1.5
NF-1	1	324 ± 67	9.8 ± 1.4	10.1 ± 6.6	90.4 ± 0.8
NF-3	3	503 ± 158	12.7 ± 2.3	6.9 ± 4.5	88.1 ± 0.8
NF-5	5	530 ± 188	13.3 ± 2.4	8.7 ± 5.9	87.9 ± 0.5
NF-10	10	422 ± 120	7.4 ± 0.7	2.9 ± 1.2	90.2 ± 0.4

^aData is the mean of 5 experimental values collected for each sample

Table 2: The percentages of biodegradation via the conversion yield of carbon in the sample to carbon dioxide according to the ASTM 5338–98 test method

Sample	Percent of degradability	
	37 ± 2°C	58 ± 2°C
Control ^a	–	–
R ⁺ ^a	92.0	100
R ⁻ ^a	0.0	0.0
NF	46.2	100

^aControl is a stable manure while R⁺ is cellulose microcrystalline and R⁻ is polyethylene sample

reduced nutrient concentration inside the granule. The early steady decay stage presented in all TCRFs released before the decay reached 0.60 fractional release (Fig. 5(b)). This phenomenon revealed the possibility that the diffusion ability of the soluble nutrient defeated the strength of the coating layer. Accordingly, the degradability of the coating layer became the crucial behavior to overcome this problem, leading to a complete nutrient release to the environment. However, the results showed a different lag time, t_{lag} , (Table 3). The coating layer thickness of TCRFs shown in Table 3 are all in the same range, 52–54 μm, due to the same resin used in the coating layer. In other words, adding B27 does not affect the thickness even at the high content of 10 wt% B27. As shown in Table 3, the t_{lag} of all TCRFs increases with increasing B27 content in the coating layer. At the 10 wt% of the B27 content, the t_{lag} decreased to 7.75 h. However, it was still higher than the 6.62 h of the original TCRF sample, containing none of the B27. The results indicated that the penetration of water to dissolve active urea molecules was slower with increasing B27 in the coating layer. This was an advantage of nanoclay role through a tortuous part of the diffusion.^{35,41} Our results were basically consistent with previous studies. In 2020, Santos et al. reported the possible reasons related to the existence of nanoclay in a polymer matrix, which is the direct effects on the retention phenomenon in the nitrogen release profile. Firstly, the

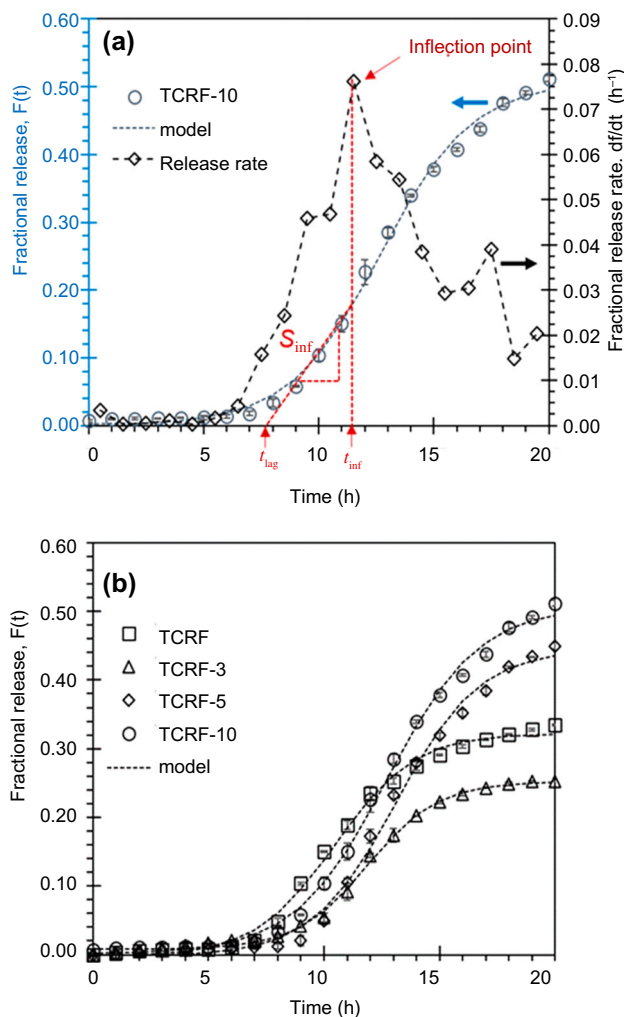


Fig. 5: Nitrogen release profiles of TCRF; (a) TCRF-10 fractional release curve including release rate and characteristic parameters definition and (b) the cumulative fractional release, $F(t)$ of TCRF series fitting with the sigmoidal kinetic pattern ($R^2 > 99\%$)

physical barrier of composite films occurred by the lamellar nanoclay in the polymer matrix, thus decreasing the solubilization rate. The second reason is that

Table 3: Kinetic parameters and diffusion coefficients of various types of TCRF

Tunable controlled-release fertilizers (TCRF)	Thickness ^a (μm)	t_{lag} (h)	t_{inf} (h)	S_{inf} (h^{-1})	D ($\mu\text{m}^2 \text{h}^{-1}$)	R^2
TCRF	52.3	6.62	8.5	0.0417	68.86	0.9961
TCRF-3	53.7	8.85	11.5	0.0450	54.31	0.9978
TCRF-5	52.3	9.32	11.5	0.0636	48.91	0.9958
TCRF-10	53.2	7.75	11.5	0.0463	60.87	0.9972

^aThe thickness value is the average of at least 20 times of at least 5 samples of each nanocomposite coated urea formula. The standard deviation is around $\pm 5 \mu\text{m}$ in all samples

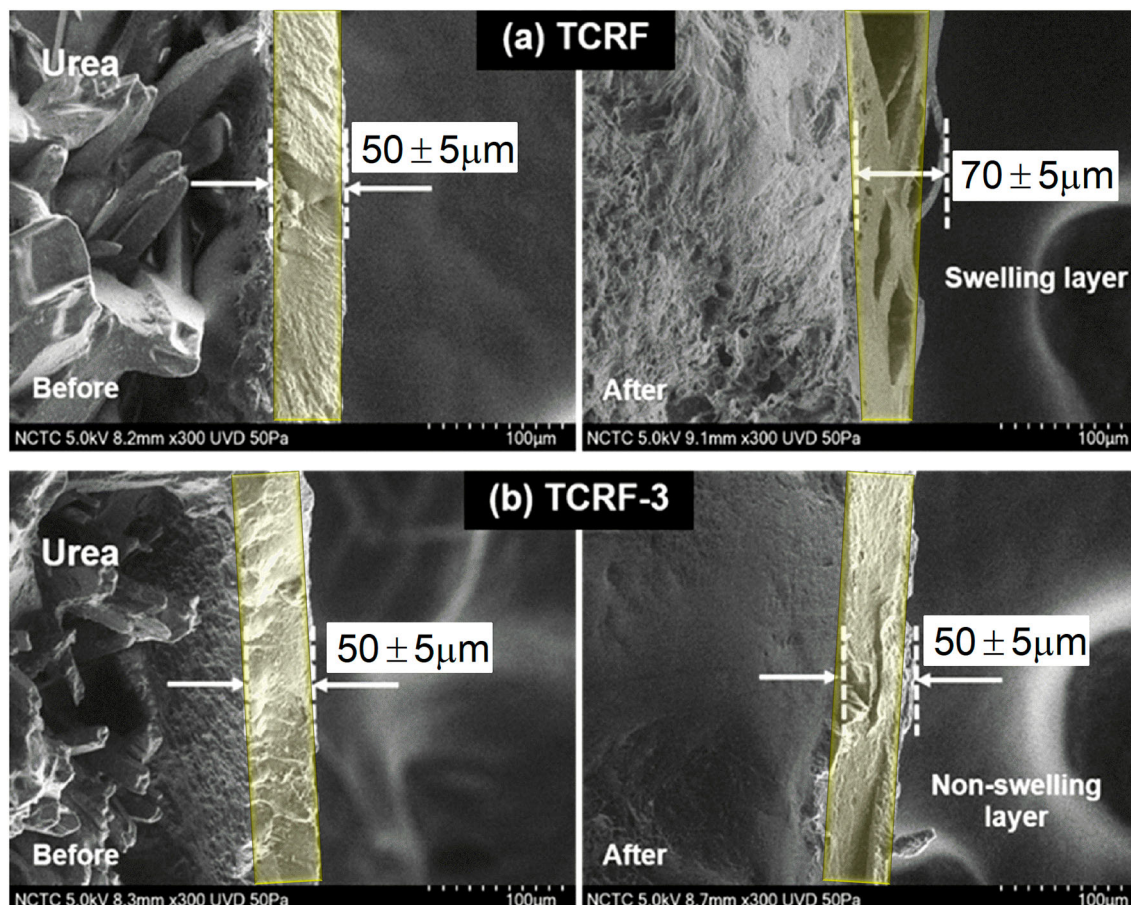


Fig. 6: Cross sectional FESEM images of (a) TCRF and (b) TCRF-3 before and after the release test. The images show different level of swelling content in the TCRF layer

the cations of nanoclay can be exchanged with another ion in its structure, leading to a promoted retention effect.¹¹ Thus, it can be indicated that the nanoclay plays an important role in improving the nutrient-tunable ability of TCRFs.

Regarding the t_{inf} , the TCRF sample also presented the lowest time compared to others, revealing an arrival to its highest release point before samples with B27. For the S_{inf} parameter, all TCRFs obtained similar values except in the TCRF-5 sample, presenting the highest constant release rate. The result may be due to the longest t_{lag} of 9.32 h, which implied a high

osmotic pressure persisted in the granule before the linear release phase occurred. For the diffusion coefficient, D , it was calculated according to the t_{lag} value and the coating thickness as mentioned in the reference (25). This character depended on the dissolution rate of the soluble nutrient and directly fluctuated with the coating thickness. The D value decreased with increasing B27 content in the coating layer from 3 to 5 wt%. However, the D raised to $60.87 \mu\text{m}^2 \text{h}^{-1}$ for the 10 wt%. Since the thickness of TCRFs were all in the same range, the t_{lag} was the main factor affecting the diffusion coefficient, D .

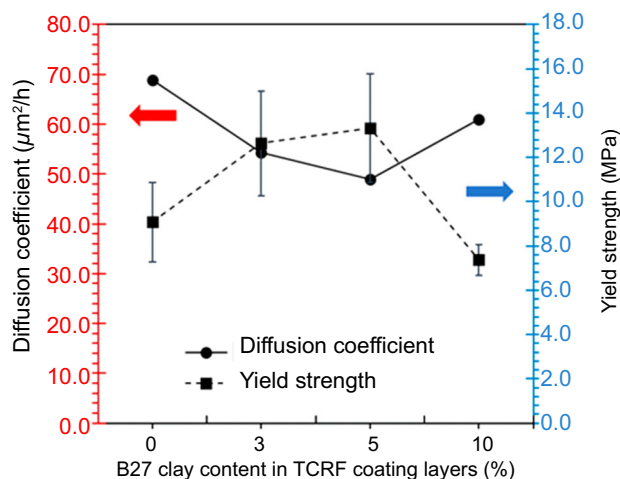


Fig. 7: Relation of TCRF series diffusion coefficients with the yield strength data of NF nanocomposite free films

Cross-sectional FESEM images of the TCRF and the TCRF-3 before and after the nitrogen release test are shown in Fig. 6. All TCRFs with an approximate 50 μm thick coating layer before the release test had similar morphologies with a clear interface between the layer and the urea core. The morphologies of the TCRF sample changed after the nitrogen release test. The TCRF, without B27 added, was swollen and separated into several sub-layers of about 70 μm thickness. This may be due to loss of layer strength during the nitrogen release test at 60°C in water. In addition, due to its high flexibility from large elongation at break of the NF shown in Table 1, the separation of layers occurred instead of cracking of the coating layer. In contrast, the coating layer of the TCRF-3 sample after the nitrogen release test still showed the non-swelling and non-separation of the coating layer. This was a result of the higher rigidity and the higher strength of the coating layer than those of the TCRF sample as shown in Table 1.

The diffusion coefficients, D , of the four TCRFs samples were an inverse relation with the yield strength as shown in Fig. 7. The relation indicated that TCRFs followed the sigmoidal release pattern and their diffusion degree depended on the strength of the coating layer. This showed the tunable controlled release property via the adjusting of the B27 concentration in the coating layer. Moreover, TCRFs contained the biodegradable polymer layer, which offered an advantage of adjustable nutrient release level of environmental friendly fertilizer that could be applied only once to suit each plant growth. A release behavior in various soil conditions and the actual field test are under investigation and a subject of a future report.

Conclusions

A tunable controlled-release urea fertilizer (TCRF) was successfully prepared using a pan coater process. The coating layer was a composite of the B27 nanoclay and the polyurethane modified long-oil alkyd resin. The B27 nanocomposite free-standing films (NFs) with varied B27 content (0, 0.5, 1, 3, 5 and 10 wt%) were studied and characterized. The NF-3 had partial exfoliated nanocomposite character according to XRD and TEM results. Mechanical properties of NFs showed increasing Young's modulus and a yield strength while decreasing elongation at break occurred with increasing B27 content. Moreover, the NF had microorganism degradability under the stable manure, which is generally used in an agricultural manner at 37 \pm 2°C and 58 \pm 2°C. Thickness of all TCRF layers were in the same range of 52–54 μm . A predictive analytic model of nitrogen release profiles at 60°C in water was found to fit well with the sigmoidal equation, which was suitable to most plant growth. Furthermore, the diffusion coefficient, D , presented an inverse trend to the yield strength of the NFs indicating that the B27 concentration played an important role to tune the release of the urea to plant and the environments. In addition, this information can be a good guideline for solving the utilization of fertilizer in agricultural applications.

Acknowledgments The authors gratefully acknowledge the fully financial support from the National Nanotechnology Center (NANOTEC), NSTDA, Thailand (Grant No. P1450077). The authors also acknowledge a technical suggestion from Assistant Professor Dr. Toemsak Srihirin (Mahidol University, Thailand), and a fruitful discussion with Professor Supapan Seraphin.

Conflict of interest The authors declare that they have no conflict of interest.

References

- Ruser, R, Flessa, H, Russow, R, Schmidt, G, Buegger, F, Munch, JC, "Emission of N₂O, N₂ and CO₂ from Soil Fertilized with Nitrate: Effect of Compaction, Soil Moisture and Rewetting." *Soil Biol. Biochem.*, **38** (2) 263–274 (2006)
- Cancellier, EL, Silva, DRG, Faquin, V, Gonçalves, BDA, Cancellier, LL, Spehar, CR, "Ammonia Volatilization from Enhanced-Efficiency Urea on No-till Maize in Brazilian Cerrado with Improved Soil Fertility." *Cienc. Agrotecnologia*, **40** (2) 133–144 (2016)

3. Raymond, JE, Fox, TR, Strahm, BD, Zerpa, J, “Ammonia Volatilization Following Nitrogen Fertilization with Enhanced Efficiency Fertilizers and Urea in Loblolly Pine (*Pinus taeda* L.) Plantations of the Southern United States.” *For. Ecol. Manag.*, **376** 247–255 (2016)
4. Mariano, E, de Sant Ana Filho, CR, Bortolettoantos, R, Bendassolli, JA, Trivelin, PCO, “Ammonia Losses Following Surface Application of Enhanced-Efficiency Nitrogen Fertilizers and Urea.” *Atmos. Environ.*, **203** 242–251 (2019)
5. Burton, DL, Zebarth, BJ, Gillam, KM, Macleod, JA, “Effect of Split Application of Fertilizer Nitrogen on N₂O Emissions from Potatoes.” *Can. J. Soil Sci.*, **88** (2) 229–239 (2008)
6. Azeem, B, Kushaari, K, Man, ZB, Basit, A, Thanh, TH, “Review on Materials & Methods to Produce Controlled Release Coated Urea Fertilizer.” *J. Control. Release*, **181** (1) 11–21 (2014)
7. Timilsena, YP, Adhikari, R, Casey, P, Muster, T, Gill, H, Adhikari, B, “Enhanced Efficiency Fertilisers: A Review of Formulation and Nutrient Release Patterns.” *J. Sci. Food Agric.*, **95** (6) 1131–1142 (2015)
8. Naz, MY, Sulaiman, SA, “Slow Release Coating Remedy for Nitrogen Loss from Conventional Urea: A Review.” *J. Control. Release*, **225** 109–120 (2016)
9. Bortoletto-Santos, R, Ribeiro, C, Polito, WL, “Controlled Release of Nitrogen-Source Fertilizers by Natural-Oil-Based Poly(Urethane) Coatings: The Kinetic Aspects of Urea Release.” *J. Appl. Polym. Sci.*, **133** (33) 1–8 (2016)
10. Bortoletto-Santos, R, Cavigelli, MA, Montes, SE, Schomberg, HH, Le, A, Thompson, AI, Kramer, M, Polito, WL, Ribeiro, C, “Oil-Based Polyurethane-Coated Urea Reduces Nitrous Oxide Emissions in a Corn Field in a Maryland Loamy Sand Soil.” *J. Clean. Prod.*, **249** 119329 (2020)
11. Bortoletto-Santos, R, Plotegher, F, Majaron, VF, da Silva, MG, Polito, WL, Ribeiro, C, “Polyurethane Nanocomposites Can Increase the Release Control in Granulated Fertilizers by Controlling Nutrient Diffusion.” *Appl. Clay Sci.*, **199** 105874–105874 (2020)
12. Niu, Y, Li, H, “Controlled Release of Urea Encapsulated by Starch-g-Poly(vinyl acetate).” *Ind. Eng. Chem. Res.*, **51** (38) 12173–12177 (2012)
13. Qiu, X, Zhu, D, Tao, S, Chen, C, Ren, X, Hu, S, “1-Naphthylacetic-Acid-Functionalized Polyacrylate-Coated Urea With Dual Controlled-Release Properties.” *J. Appl. Polym. Sci.*, **129** (2) 559–567 (2013)
14. Zhao, Z, Verburg, K, Huth, N, “Modelling Sugarcane Nitrogen Uptake Patterns to Inform Design of Controlled Release Fertiliser for Synchrony of N Supply and Demand.” *Field Crops Res.*, **213** (April) 51–64 (2017)
15. Tian, X, Li, C, Zhang, M, Li, T, Lu, Y, Liu, L, “Controlled Release Urea Improved Crop Yields and Mitigated Nitrate Leaching under Cotton-Garlic Intercropping System in a 4-Year Field Trial.” *Soil Tillage Res.*, **175** 158–167 (2018)
16. Kumar, K, Goh, KM, “Recovery of 15N-Labelled Fertilizer Applied to Winter Wheat and Perennial Ryegrass Crops and Residual 15N Recovery by Succeeding Wheat Crops Under Different Crop Residue Management Practices.” *Nutr. Cycl. Agroecosystems*, **62** (2) 123–130 (2002)
17. Zhu, S, Vivanco, JM, Manter, DK, “Nitrogen Fertilizer Rate Affects Root Exudation, the Rhizosphere Microbiome and Nitrogen-use-Efficiency of Maize.” *Appl. Soil Ecol.*, **107** 324–333 (2016)
18. Simpson, J, Warren, C, Adams, P, “Potential Protease Activity and Organic Nitrogen Concentration are Rapid Tests and Accurate Indicators of N-Availability in Tasmanian *Eucalyptus nitens* Plantations.” *Soil Biol. Biochem.*, **115** 152–160 (2017)
19. Rodeghiero, M, Vesterdal, L, Marcolla, B, Vescovo, L, Aertens, W, Martinez, C, Di Cosmo, L, Gasparini, P, Gianelle, D, “Soil Nitrogen Explanatory Factors Across a Range of Forest Ecosystems and Climatic Conditions in Italy.” *For. Ecol. Manag.*, **408** 25–35 (2018)
20. Al-Zahrani, SM, “Controlled-Release of Fertilizers: Modelling and Simulation.” *Int. J. Eng. Sci.*, **37** (10) 1299–1307 (1999)
21. Melaj, MA, Daraio, ME, “HPMC Layered Tablets Modified with Chitosan and Xanthan as Matrices for Controlled-Release Fertilizers.” *J. Appl. Polym. Sci.*, **131** (19) 1–7 (2014)
22. Rizwan, M, Gilani, SR, Durrani, AI, Naseem, S, “Kinetic Model Studies of Controlled Nutrient Release and Swelling Behavior of Combo Hydrogel Using Acer Platanoides Cellulose.” *J. Taiwan Inst Chem Eng*, **131** 104137 (2022)
23. Sempeho, SI, Kim, HT, Mubofu, E, Hilonga, A, “Meticulous Overview on the Controlled Release Fertilizers.” *Adv. chem. sci.*, **2014** 1–16 (2014)
24. Lubkowski, K, Smorowska, A, Grzmil, B, Kozłowska, A, “Controlled-Release Fertilizer Prepared Using a Biodegradable Aliphatic Copolyester of Poly(butylene succinate) and Dimerized Fatty Acid.” *J. Agric. Food Chem.*, **63** (10) 2597–2605 (2015)
25. Trinh, TH, Kushaari, K, Shuib, AS, Ismail, L, Azeem, B, “Modelling the Release of Nitrogen from Controlled Release Fertiliser: Constant and Decay Release.” *Biosyst. Eng.*, **130** 34–42 (2015)
26. Shaviv, A, Raban, S, Zaidel, E, “Modeling Controlled Nutrient Release from Polymer Coated Fertilizers: Diffusion Release from Single Granules.” *Environ. Sci. Technol.*, **37** (10) 2251–2256 (2003)
27. Shaviv, A, Raban, S, Zaidel, E, “Modeling Controlled Nutrient Release from a Population of Polymer Coated Fertilizers: Statistically Based Model for Diffusion Release.” *Environ. Sci. Technol.*, **37** (10) 2257–2261 (2003)
28. Du, CW, Zhou, JM, Shaviv, A, “Release Characteristics of Nutrients from Polymer-Coated Compound Controlled Release Fertilizers.” *J Polym Environ.*, **14** (3) 223–230 (2006)
29. Tan, B, Thomas, NL, “A Review of the Water Barrier Properties of Polymer/Clay and Polymer/Graphene Nanocomposites.” *J. Membr. Sci.*, **514** 595–612 (2016)
30. Zabihi, O, Ahmadi, M, Nikafshar, S, Chandrakumar Preyeswary, K, Naebe, M, “A Technical Review on Epoxy-Clay Nanocomposites: Structure, Properties, and Their Applications in Fiber Reinforced Composites.” *Compos. B. Eng.*, **135** 1–24 (2018)
31. Ni, B, Lu, S, Liu, M, “Novel Multinutrient Fertilizer and its Effect on Slow Release, Water Holding, and Soil Amending.” *Ind. Eng. Chem. Res.*, **51** (40) 12993–13000 (2012)
32. Roshanravan, B, Soltani, SM, Mahdavi, F, Rashid, SA, Yusop, MK, “Preparation of Encapsulated Urea-Kaolinite Controlled Release Fertiliser and Their Effect on Rice Productivity.” *Chem. Speciat. Bioavailab.*, **26** (4) 249–256 (2014)
33. Uzoh CF, Odera, SR “Lag, Constant and Decay Release Characteristic of St-PVOH Encapsulated Urea as a Function of Coating Thickness Using Different Empirical Models.” In: *Microencapsulation - Processes, Technologies and Industrial Applications*. IntechOpen Publishers pp.1–14 (2019)
34. Ito, R, Golman, B, Shinohara, K, “Design of Multi-Layer Coated Particles with Sigmoidal Release Pattern.” *Chem. Eng. Sci.*, **60** (20) 5415–5424 (2005)
35. Lee, SM, Tiwari, D, “Organo and Inorgano-Organo-Modified Clays in the Remediation of Aqueous Solutions: An Overview.” *Appl. Clay Sci.*, **59–60** 84–102 (2012)

36. Saha, C, Chaki, TK, Singha, NK, “Synthesis and Characterization of Elastomeric Polyurethane and PU/Clay Nanocomposites Based on an Aliphatic Diisocyanate.” *J. Appl. Polym. Sci.*, **130** (5) 3328–3334 (2013)
37. Ferfera-Harrar, H, Dairi, N, “Green Nanocomposite Films Based on Cellulose Acetate and Biopolymer-Modified Nanoclays: Studies on Morphology and Properties.” *IRAN POLYM J.*, **23** (12) 917–931 (2014)
38. Silva, AA, Soares, BG, Dahmouche, K, “Organoclay-Epoxy Nanocomposites Modified with Polyacrylates: The Effect of the Clay Mineral Dispersion Method.” *Appl. Clay Sci.*, **124–125** 46–53 (2016)
39. Jia, X, Ma, ZY, Zhang, GX, Hu, JM, Liu, ZY, Wang, HY, Zhou, F, “Polydopamine Film Coated Controlled-Release Multielement Compound Fertilizer Based on Mussel-Inspired Chemistry.” *J. Agric. Food Chem.*, **61** (12) 2919–2924 (2013)
40. Barbanti, L, Grandi, S, Vecchi, A, Venturi, G, “Sweet and Fibre Sorghum (*Sorghum bicolor* (L.) Moench), Energy Crops in the Frame of Environmental Protection from Excessive Nitrogen Loads.” *Eur. J. Agron.*, **25** (1) 30–39 (2006)
41. Mondal, D, Bhowmick, B, Mollick, MMR, Maity, D, Mukhopadhyay, A, Rana, D, Chattopadhyay, D, “Effect of Clay Concentration on Morphology and Properties of Hydroxypropylmethylcellulose Films.” *Carbohydr. Polym.*, **96** (1) 57–63 (2013)

Publisher’s Note Springer Nature remains neutral with regard to jurisdictional claims in published maps and institutional affiliations.

Springer Nature or its licensor holds exclusive rights to this article under a publishing agreement with the author(s) or other rightsholder(s); author self-archiving of the accepted manuscript version of this article is solely governed by the terms of such publishing agreement and applicable law.